


Template-Induced Precursor Formation in Heterogeneous Nucleation: Controlling Polymorph Selection and Nucleation Efficiency

Grisell Díaz Leines¹**Yusuf Hamied Department of Chemistry, University of Cambridge, Cambridgeshire CB2 1EW, United Kingdom*Jutta Rogal²*Department of Chemistry, New York University, New York, New York 10003, USA and Fachbereich Physik, Freie Universität Berlin, 14195 Berlin, Germany* (Received 26 June 2021; accepted 29 March 2022; published 19 April 2022)

We present an atomistic study of heterogeneous nucleation in Ni employing transition path sampling, which reveals a template precursor-mediated mechanism of crystallization. Most notably, we find that the ability of tiny templates to modify the structural features of the liquid and promote the formation of precursor regions with enhanced bond-orientational order is key to determining their nucleation efficiency and the polymorphs that crystallize. Our results reveal an intrinsic link between structural liquid heterogeneity and the nucleating ability of templates, which significantly advances our understanding toward the control of nucleation efficiency and polymorph selection.

DOI: [10.1103/PhysRevLett.128.166001](https://doi.org/10.1103/PhysRevLett.128.166001)

Gaining control on the emerging polymorphs during crystal nucleation is of crucial importance for the synthesis and design of nanomaterials with targeted properties. The presence of impurities and interfaces significantly modifies induction times and the selection of preferred polymorphs during crystallization, which has fuelled extensive research that focuses on understanding what determines the nucleating ability of a template [1–9]. Yet, unraveling the kinetic pathways of crystal nucleation at the nanoscale poses a major challenge [10] as many systems exhibit complex transitions, and often nontrivial microscopic correlations between liquid-surface interactions and template morphologies are observed, leaving the problem largely unsolved. Fundamental knowledge on template-driven nucleation mechanisms is of key importance to shed light on predictive rules that allow for better control of crystallization processes.

Longstanding views on heterogeneous nucleation generally propose that the presence of a template influences the nucleation mechanism to a degree in which the template is commensurate with the growing solid cluster in both density and symmetry [11]. However, it is well documented that a small lattice mismatch, although an important factor, is often not the sole requirement for an efficient and successful crystal template. Other factors, like template morphology, absorption, and the local ordering of the contact liquid layer can also largely impact the nucleation mechanisms [3,9,12–14]. Yet, our current fundamental knowledge on the key factors that determine the nucleating ability of a template is far from conclusive and remains unsatisfactory to date.

Recent evidence demonstrating the formation of crystalline precursors in the liquid that promote the nucleation

of preselected polymorphs [15–20] has raised great interest in understanding the impact of structural and dynamical heterogeneity in the supercooled liquid on the crystallization mechanism. Precursor-induced crystallization processes, often referred to as two-step nucleation mechanisms, are characterized by the initial formation of preordered regions in the liquid that exhibit changes in bond-orientational order, density, or mobility, and facilitate the formation of crystal nuclei, presumably by decreasing the crystal-liquid interfacial free energy [21–23]. Russo *et al.* [20] showed that preordered regions in hard sphere liquids act as polymorph precursors by preselecting the polyhedra with the closest symmetry to those of the crystalline phases that nucleate. Previously, we have shown that preordered liquid regions also act as preferred nucleation sites that predetermine the polymorphs in metallic systems with face-centered cubic (fcc) [21,24] and body-centered cubic (bcc) [25] bulk structures. Several studies on nucleation of ice [26] metals [21,24,27], hard spheres [28,29], and colloidal models [30,31] have corroborated an existing link between liquid heterogeneity and the enhancement of the nucleation probability, as well as the selection of polymorphs during the first stages of crystallization. Indeed, a recent work on model binary liquids with tunable glass-forming ability [23] showed that the structural differences within the supercooled liquids are key to controlling the glass and crystal-forming ability. Fundamental knowledge of the relation between structural and dynamical heterogeneity of supercooled liquids and nucleation is therefore opening up a new perspective in our understanding of crystallization mechanisms and providing novel possibilities to control polymorph outcomes. Yet, it is largely unexplored how

nucleating agents and interfaces impact the structural and dynamical characteristics of the supercooled liquid, and how this is connected with heterogeneous nucleation mechanisms.

In this Letter, we tackle the above question by investigating how small seeds with different crystal structures modify the structural characteristics of the supercooled liquid and ultimately impact the crystallization mechanism. The importance of studying small seeds to improve our understanding of crystallization mechanisms and toward the selective control of materials properties, has been made evident in [3,4,32–35]. Experimentally, this can be achieved with optical tweezers [36–40] where templates are created by fixing the positions of atoms in the liquid to investigate the impact on the polymorphs that crystallize and the rates. Our study focuses on Ni, for which we have previously identified strong spacial-temporal correlations between preordered liquid regions and the nucleation process [21,24]. The role of liquid preordering during template-driven crystallization in Ni is, however, unknown. To enable an efficient sampling of the nucleation process, we employ transition interface sampling (TIS) [41–43]. In TIS, an unbiased ensemble of all possible nucleation pathways between the solid and liquid state [42–44] is computed. Kinetic and dynamical properties, such as nucleation barriers and rate constants, can be obtained by reweighting each path in the ensembles according to its correct probability [44]. Our analysis of heterogeneous nucleation pathways reveals a novel template-driven mechanism, where the ability of the seeds to enhance the nucleation probability of selected polymorphs is not directly determined by the degree of lattice mismatch between the seeds and the crystalline bulk phase, but by their ability to promote the formation of precursor regions that modify the nucleation probability and facilitate the emergence of specific polymorphs.

All simulations were performed in the NPT ensemble employing an embedded atom method potential for Ni [45] and the LAMMPS code [46] as molecular dynamics (MD) driver together with a PYTHON wrapper for the TIS simulations [computational details in Supplemental Material (SM) [47]]. To discriminate between solidlike and liquidlike particles, the approach introduced by ten Wolde and Frenkel [52,53] was used (details in SM [47]). The size of the largest solid cluster n_s is determined via a clustering algorithm. For the local identification of crystal structures such as fcc, hexagonal close-packed (hcp), bcc, as well as liquid and prestructured liquid, we use averaged Steinhardt parameters [54] \bar{q}_4, \bar{q}_6 . *Prestructured liquid* particles are particles that exhibit higher bond-orientational order than the liquid, but less than any of the crystalline phases and fall outside the corresponding regions on the \bar{q}_4, \bar{q}_6 map (Fig. 1). Details can be found in Ref. [24] and in SM [47].

In order to associate the nucleating ability of templates with the formation of efficient precursors in the melt, we first investigate the structural characteristics of preordered

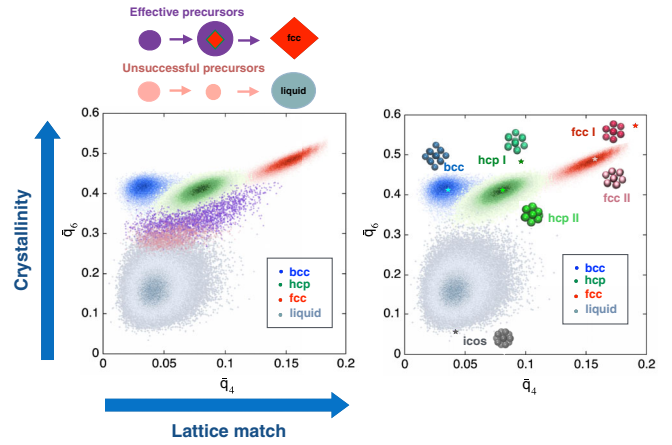


FIG. 1. Left: $\bar{q}_4 - \bar{q}_6$ values for preordered liquid particles in precritical clusters ($n_s = 50$) of the TPE that reach critical size and crystallize (purple dots), and in the precritical clusters of smaller sizes that commit back to the liquid phase (pink dots). Left top: Schematic representation of preordered liquid clusters with higher bond-orientational order (purple) that crystallize and lower bond-orientational order (pink) that melt. Right: $\bar{q}_4 - \bar{q}_6$ values of selected seeds with different structures.

regions in the liquid that act as preferential sites for homogeneous nucleation in Ni. To this end, we analyze precritical clusters obtained from 400 trajectories of the transition path ensemble (TPE) of homogeneous nucleation in Ni [21,24] at $\Delta T/T_m = 20\%$ undercooling. In the crystallization mechanism found in pure Ni [24], precritical clusters with $n_s \leq 50$ are mostly composed of prestructured liquid (> 90%) and facilitate the subsequent nucleation of crystallites within the core of these precursor regions [24]. Thus, for our analysis of precursors, we harvest precritical clusters with $n_s = 50$ from 400 trajectories of the reweighted path ensemble (RPE). The left graph in Fig. 1 shows a reference \bar{q}_4, \bar{q}_6 map of the crystalline phases and the liquid together with the distribution of \bar{q}_4, \bar{q}_6 values of prestructured liquid particles in these precritical clusters from trajectories that successfully nucleate into the crystal phase (purple), in comparison to clusters that become unstable and dissolve (pink). The prestructured liquid clusters that continue to grow beyond the critical size exhibit a clear increase in bond-orientational order. Furthermore, preordered clusters that serve as nucleation sites tend to contain hcp-like and fcc-like structural motifs, resembling the bulk structure that crystallizes. In contrast, precritical clusters that dissolve are characterized by lower bond-orientational order with structural features closer to the liquid. Therefore, *effective* precursor regions with higher bond-orientational order and hcp-like and fcc-like features in the liquid template crystal nucleation by providing preferential sites for critical fluctuations.

Having established that fluctuations in the liquid with higher \bar{q}_4, \bar{q}_6 values promote crystallization during homogeneous nucleation, we investigate how small Ni seeds with

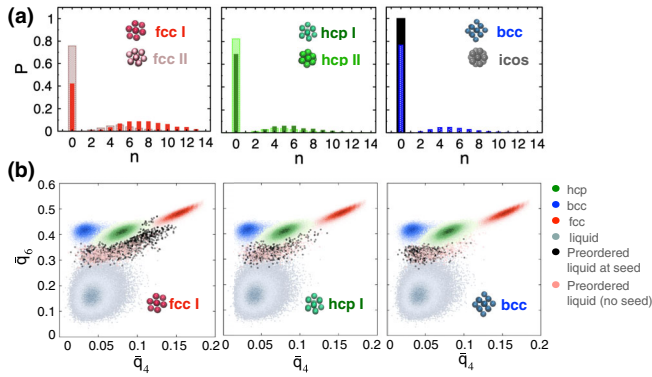


FIG. 2. (a) Frequency of the formation of preordered clusters at the seed in supercooled liquid. Shown is the number of atoms n of the seed that belong to the largest preordered cluster that emerges during fluctuations in the supercooled liquid, at $\Delta T/T_m = 0.20$. (b) $\bar{q}_4 - \bar{q}_6$ values for preordered liquid particles that belong to the largest precritical cluster that emerges within homogeneous liquid (pink) and at selected seeds (black) in the liquid. Additional distributions for all other seeds are shown in SM [47].

different crystal structures modify the structural features of the liquid and the crystal precursors, in connection with their nucleating ability. We select seeds with fcc, bcc, hcp, and icosahedral structures and various degrees of crystallinity, as shown in the \bar{q}_4, \bar{q}_6 map in Fig. 1 (right). The tiny seeds consist of atoms within the first coordination polyhedron. We include two types of fcc and hcp seeds, labeled as fcc I and hcp I, and fcc II and hcp II, respectively, which have the same symmetry and average bond length but differ in crystallinity. Fcc I and hcp I correspond to perfect polyhedra, while fcc II and hcp II represent polyhedra with thermal distortions. The seeds are inserted in the liquid and have a fixed position. To test the approximation of fixed seeds, we have also performed simulations with an fcc seed that is allowed to vibrate, yielding comparable results (see SM [47]).

We first characterize the ability of the seeds to promote the formation of preordered regions in the liquid that emerge from precritical fluctuations (typically $n_s < 30$), by considering two aspects: (i) the frequency of formation of the largest prestructured liquid cluster at the seed, and (ii) the degree of bond-orientational order and the structural hallmarks of the prestructured regions formed at the seed. To address these two aspects, we perform five independent MD simulations of liquid Ni over 5 ns at $\Delta T/T_m = 0.20$ for each seed. The distribution of the number of seed atoms that belong to the largest prestructured liquid cluster is shown in Fig. 2(a), the \bar{q}_4, \bar{q}_6 values of the preordered clusters that emerge at the seed in Fig. 2(b) (results for other seeds shown in SM [47]). If none of the seed atoms are included in the prestructured cluster ($n = 0$), precritical fluctuations occur far from the seed. This is further supported by evaluating the distribution of minimum distances between the seed and the largest prestructured

cluster (see SM [47]). Our results show that the most commensurate seeds with larger bond-orientational order (fcc I) clearly promote more frequent precritical fluctuations of preordered clusters at the seed [Fig. 2(a)] and enhance the crystallinity and fcc-like symmetries in the prestructured liquid, in comparison to preordered regions found in homogeneous liquid [Fig. 2(b)]. Indeed, for the fcc I seed, 60% of the preordered clusters form at the seed, while for hcp I and fcc II seeds, with lower crystallinity, 34% and 24% of the preordered clusters form at the seed, respectively. For hcp II and bcc seeds, which are expected to be less efficient nucleating agents, only 12% and 18% of the preordered clusters emerge at the seed, respectively, while precritical fluctuations always occur far from the icosahedral seed, indicating that preordering in the liquid is inhibited in its vicinity. Overall, we observe that seeds with larger crystallinity promote an increase in crystallinity and fcc-like structural features in the precursors, as evidenced by the shift in the distributions in Fig. 2(b). In contrast, seeds with lower crystallinity (bcc and hcp II) promote hcp and bcc-like preordering in the liquid with negligible increase in bond-orientational order. It is also interesting to note that, although fcc I, fcc II, and the vibrating fcc seed (see SM [47]), as well as hcp I and II share a common crystal structure, their variation in crystallinity results in significant differences in the frequency of formation of precursors at the seed and the structural features of these regions. Indeed, seeds with the potential to promote frequent formation of preordered clusters with high crystallinity and fcc-like order in the liquid are bound to enhance the formation of *effective* precursors, i.e., preordered regions which become active sites for nucleation, and, presumably, such seeds exhibit a larger nucleating ability.

In order to establish the connection between structural changes in the liquid induced by the seeds and the nucleation mechanisms, we performed TIS simulations for all seeds (computational details in SM [47]). In all cases, the analysis of the structural compositions of the growing nuclei in the TPE (see SM [47]) reveals a precursor-induced crystallization mechanism, similar to the one found in homogeneous nucleation [24], where we find a prestructured region of long life that is present before the crystal clusters nucleate. An analysis of the spatial location of the seeds within solid clusters of precritical and critical sizes (see SM [47]) shows that if a seed is part of the growing nucleus, a preordered liquid cluster initially forms at the seed and grows in its surroundings. As the cluster reaches critical size, the seed remains predominantly located at the surface of the nucleus, where it is surrounded mostly by prestructured liquid atoms and random hcp (see movie of nucleation trajectory in SM [47]). These findings strongly suggest that the seeds impact the nucleation probability and mechanism by promoting the initial formation of precursors in the supercooled liquid instead of directly templating the formation of the crystalline phase. Indeed, if the nucleation events at the seeds were

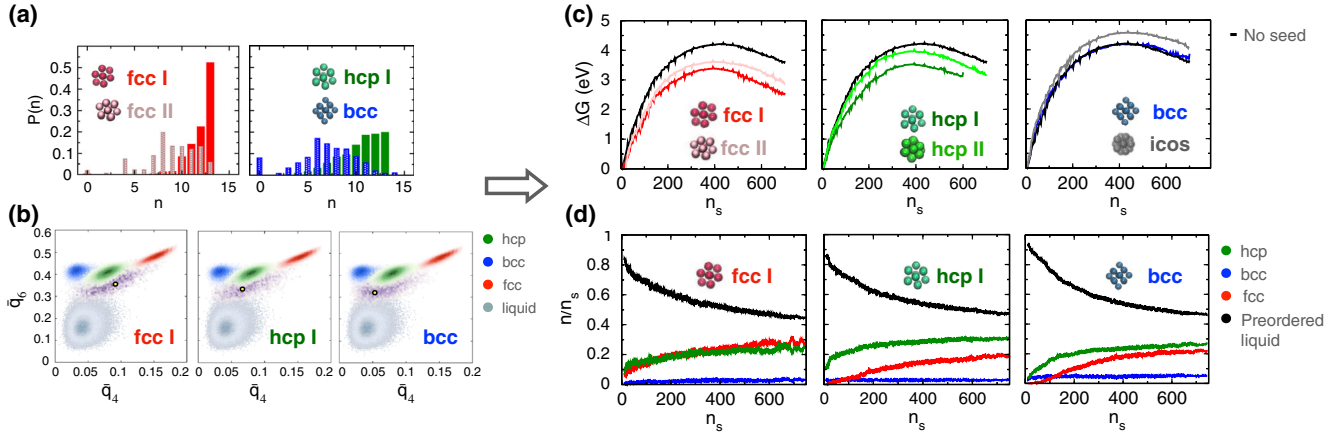


FIG. 3. (a) Distributions of the number of seed atoms n included in precritical clusters ($n_s = 50$) that successfully grow and crystallize (effective precursors). The precritical configurations were obtained from the TPE. (b) \bar{q}_4, \bar{q}_6 distributions of the effective precursors in the presence of different seeds. The yellow circle indicates the maximum of the distribution. (c) Free energy profiles $\Delta G(n_s)$ and nucleation barriers for crystallization in the presence of various seeds, in comparison to homogeneous nucleation in Ni. (d) Structural composition of the growing nucleus in the presence of various seeds.

driven solely by the initial enhancement of translational order, we would rather expect fcc crystallites to nucleate right at the seeds without an intermediate precursor and, consequently, the seeds to be located in the core of the critical clusters. Therefore, the overall efficiency of a seed to promote nucleation events and, in general, to modify the nucleation mechanism can be characterized by (i) the ability to promote the formation of *effective* precursors, (ii) the potential to reduce the free energy barrier, and (iii) the propensity to template the formation of favorable polymorphs.

We assess these three aspects for all seeds by analyzing configurations from at least 500 liquid-solid pathways in the TPE. Figure 3(a) shows the distributions of the number of seed atoms n included in *effective* precursors of precritical size ($n_s = 50$), that is preordered clusters that successfully grow and crystallize. Seeds with the highest crystallinity and commensurability, such as fcc I and II, are part of the growing clusters for 99% of the solid-liquid pathways and thus successfully promote nucleation events at the seed. For other seeds with lower crystallinity and commensurability (hcp I, hcp II, bcc), there is a stronger competition between heterogeneous and homogeneous nucleation pathways. In case of hcp I seeds, these two pathways appear to follow separate channels which results in a strong dependency of the TPE on the initial trajectory. If the hcp I seed is initially part of the crystal cluster, the TPE is predominantly composed of heterogeneous nucleation pathways while initial paths with the hcp I seed far from the growing cluster result in a TPE with predominantly homogeneous nucleation pathways. The overall nucleation mechanism in the presence of hcp I seeds would be given by a properly weighted average of the two pathways. Icosahedral seeds are never identified as part of the growing cluster, implying that nucleation occurs

mostly far away from the seeds. Interestingly, the distributions are noticeably different for all the seeds, even for those with shared crystal structures: while seeds with high crystallinity, such as fcc I, are mostly included in the clusters ($n > 10$), partial attachment of the crystalline clusters to other seeds with lower crystallinity (fcc II, hcp II, bcc) is more frequently observed ($n < 6$), implying significant variations in the ability of the seeds to promote the formation of *effective* precursors. These results are consistent with our findings for precritical fluctuations shown in Fig. 2(a).

The ability to promote *effective* precursors is further assessed by analyzing the distributions of \bar{q}_4, \bar{q}_6 values of the precritical clusters ($n_s = 50$) that successfully grow and crystallize at the seeds. The shift and spread in the distributions of \bar{q}_4, \bar{q}_6 values shown in Fig. 3(b) clearly illustrates that prestructured liquid atoms in precursors that form at seeds with higher crystallinity (fcc I) display a significant increase in bond-orientational order and fcc-like ordering [marked with a yellow circle in Fig. 3(b)]. This change in the structural characteristics of the preordered region is likely to reduce induction times and enhance nucleation rates in comparison to other seeds and homogeneous nucleation. Correspondingly, the fcc I seed reduces the free energy barrier significantly by ~ 0.85 eV compared to homogeneous nucleation with $\Delta G_{\text{homo}}^* = 4.21$ eV [Fig. 3(c)]. The less effective fcc II and hcp I seeds, with comparable crystallinity, reduce the nucleation barrier extracted from heterogeneous nucleation pathways by only ~ 0.6 and ~ 0.69 eV, respectively. The hcp II and bcc seeds enhance bond-orientational order in the precursors only minimally and, thus, the free energy barriers are comparable to homogeneous nucleation. Interestingly, the nucleation barrier at the icosahedral seed is even increased, implying that this seed acts as an impurity that reduces the

nucleation capability in Ni. Icosahedral seeds inhibit the formation of preordered regions in their surrounding, thus resulting in excluded volume for nucleation sites.

The impact of the seeds on the formation of different polymorphs is evaluated by analyzing the average structural composition of the growing nuclei shown in Fig. 3(d). The polymorphs selected during crystal nucleation in Ni correlate strongly with the structural hallmarks promoted by the seeds in the preordered liquid. The fcc I and II seeds promote the formation of precursors with enhanced fcc-like hallmarks and, consequently, yield a rapid and predominant emergence of fcc crystallites within the cores of the crystal precursors and critical nuclei [Fig. 3(d) and SM [47]]. In contrast, for hcp I, hcp II, and bcc seeds, which promote the formation of precursors with hcp-like hallmarks, we find a larger fraction of hcp crystallites that compete with fcc.

In contrast to the assumptions of classical nucleation theory, where random fluctuations of order within the homogeneous liquid yield crystallization, we have shown that supercooled liquids exhibit structural heterogeneity that can be linked directly to crystal nucleation and to the ability of templates to enhance the nucleation probability and modify the polymorphs. We propose a novel heterogeneous nucleation mechanism, where the nucleating ability of tiny seeds and the selection of polymorphs is not only determined by the lattice match and translational order of the templates, but is strongly linked to the ability of the seeds to promote the formation of precursors in the liquid with enhanced bond-orientational order and favorable structural hallmarks. Previous findings of precursor-mediated crystallization mechanisms in a large variety of systems [14,21,22,24,27–31] suggest that this novel perspective of heterogeneous nucleation could be of relevance for other materials. Our results open new venues to understand and control template-driven crystallization and polymorph selection.

We acknowledge financial support by the German Research Foundation (DFG) through Project No. 262052203 and the DFG Heisenberg Programme Project No. 428315600. G.D.L. acknowledges support from Conacyt-Mexico through Fellowship No. 220644 and from the Isaac Newton Trust Grant No. 20.40(h). The authors acknowledge computing time by the Center for Interface-Dominated High Performance Materials (ZGH, Ruhr-Universität Bochum, Germany).

*gd466@cam.ac.uk

- [1] G. C. Sosso, J. Chen, S. J. Cox, M. Fitzner, P. Pedevilla, A. Zen, and A. Michaelides, Crystal nucleation in liquids: Open questions and future challenges in molecular dynamics simulations, *Chem. Rev.* **116**, 7078 (2016).
- [2] E. M. Pouget, P. H. H. Bomans, J. A. C. M. Goos, P. M. Frederik, G. de With, and N. A. J. M. Sommerdijk, The initial stages of template-controlled CaCO₃ formation revealed by Cryo-TEM, *Science* **323**, 1455 (2009).
- [3] S. Jungblut and C. Dellago, Crystallization on prestructured seeds, *Phys. Rev. E* **87**, 012305 (2013).
- [4] A. Cacciuto, S. Auer, and D. Frenkel, Onset of heterogeneous crystal nucleation in colloidal suspensions, *Nature (London)* **428**, 404 (2004).
- [5] Y. Chen, Z. Yao, S. T. Tang, H., T. Yanagishima, H. Tanaka, and P. Tan, Morphology selection kinetics of crystallization in a sphere, *Nat. Phys.* **17**, 121 (2021).
- [6] J. V. Parambil, S. K. Poornachary, J. Y. Y. Heng, and R. B. H. Tan, Template-induced nucleation for controlling crystal polymorphism: From molecular mechanisms to applications in pharmaceutical processing, *CrystEngComm* **21**, 4122 (2019).
- [7] E. Allahyarov, K. Sandomirski, S. Egelhaaf, and H. Löwen, Crystallization seeds favour crystallization only during initial growth, *Nat. Commun.* **6**, 7110 (2015).
- [8] S. Jungblut and C. Dellago, Pathways to self-organization: Crystallization via nucleation and growth, *Eur. Phys. J. E* **39**, 77 (2016).
- [9] M. Fitzner, P. Pedevilla, and A. Michaelides, Predicting heterogeneous ice nucleation with a data-driven approach, *Nat. Commun.* **11**, 4777 (2020).
- [10] D. Blow, K. E. Quigley, and G. C. Sosso, The seven deadly sins: When computing crystal nucleation rates, the devil is in the details, *J. Chem. Phys.* **155**, 040901 (2021).
- [11] D. Turnbull and B. Vonnegut, Nucleation catalysis, *Ind. Eng. Chem.* **44**, 1292 (1952).
- [12] G. I. Tóth, G. Tegze, T. Pusztai, and L. Gránásy, Heterogeneous Crystal Nucleation: The Effect of Lattice Mismatch, *Phys. Rev. Lett.* **108**, 025502 (2012).
- [13] A. J. Page and R. P. Sear, Crystallization controlled by the geometry of a surface, *J. Am. Chem. Soc.* **131**, 17550 (2009).
- [14] L. Lupi, B. Peters, and V. Molinero, Pre-ordering of interfacial water in the pathway of heterogeneous ice nucleation does not lead to a two-step crystallization mechanism, *J. Chem. Phys.* **145**, 211910 (2016).
- [15] D. Gebauer, M. Kellermeier, J. D. Gale, L. Bergström, and H. Cölfen, Pre-nucleation clusters as solute precursors in crystallisation, *Chem. Soc. Rev.* **43**, 2348 (2014).
- [16] P. R. ten Wolde and D. Frenkel, Enhancement of protein crystal nucleation by critical density fluctuations, *Science* **277**, 1975 (1997).
- [17] P. R. ten Wolde and D. Frenkel, Homogeneous nucleation and the Ostwald step rule, *Phys. Chem. Chem. Phys.* **1**, 2191 (1999).
- [18] T. Zhang and X. Y. Liu, How does a transient amorphous precursor template crystallization, *J. Am. Chem. Soc.* **129**, 13520 (2007).
- [19] S. Prestipino, A. Laio, and E. Tosatti, Systematic Improvement of Classical Nucleation Theory, *Phys. Rev. Lett.* **108**, 225701 (2012).
- [20] J. Russo and H. Tanaka, The microscopic pathway to crystallization in supercooled liquids, *Sci. Rep.* **2**, 505 (2012).
- [21] G. Díaz Leines and J. Rogal, Maximum likelihood analysis of reaction coordinates during solidification in Ni, *J. Phys. Chem. B* **122**, 10934 (2018).

- [22] H. Tanaka, Bond orientational order in liquids: Towards a unified description of water-like anomalies, liquid-liquid transition, glass transition, and crystallization, *Eur. Phys. J. E* **35**, 113 (2012).
- [23] J. Russo, F. Romano, and H. Tanaka, Glass Forming Ability in Systems with Competing Orderings, *Phys. Rev. X* **8**, 021040 (2018).
- [24] G. Díaz Leines, R. Drautz, and J. Rogal, Atomistic insight into the non-classical nucleation mechanism during solidification in Ni, *J. Chem. Phys.* **146**, 154702 (2017).
- [25] S. Menon, G. Díaz Leines, R. Drautz, and J. Rogal, Role of pre-ordered liquid in the selection mechanism of crystal polymorphs during nucleation, *J. Chem. Phys.* **153**, 104508 (2020).
- [26] M. Fitzner, G. C. Sosso, S. J. Cox, and A. Michaelides, Ice is born in low-mobility regions of supercooled liquid water, *Proc. Natl. Acad. Sci. U.S.A.* **116**, 2009 (2019).
- [27] Q. Zhang, J. Wang, S. Tang, Y. Wang, J. Li, W. Zhou, and Z. Wang, Molecular dynamics investigation of the local structure in iron melts and its role in crystal nucleation during rapid solidification, *Phys. Chem. Chem. Phys.* **21**, 4122 (2019).
- [28] T. Schilling, H. J. Schöpe, M. Oettel, G. Opletal, and I. Snook, Precursor-Mediated Crystallization Process in Suspensions of Hard Spheres, *Phys. Rev. Lett.* **105**, 025701 (2010).
- [29] H. J. Schöpe, G. Bryant, and W. van Meegen, Two-Step Crystallization Kinetics in Colloidal Hard-Sphere Systems, *Phys. Rev. Lett.* **96**, 175701 (2006).
- [30] W. Lechner, C. Dellago, and P. G. Bolhuis, Role of the Prestructured Surface Cloud in Crystal Nucleation, *Phys. Rev. Lett.* **106**, 085701 (2011).
- [31] P. Tan, N. Xu, and L. Xu, Visualizing kinetic pathways of homogeneous nucleation in colloidal crystallization, *Nat. Phys.* **10**, 73 (2014).
- [32] V. W. A. de Villeneuve, D. Verboekend, R. P. A. Dullens, D. G. A. L. Aarts, W. K. Kegel, and H. N. W. Lekkerkerker, Hard sphere crystal nucleation and growth near large spherical impurities, *J. Phys. Condens. Matter* **17**, S3371 (2005).
- [33] S. Jungblut and C. Dellago, Heterogeneous crystallization on tiny clusters, *Europhys. Lett.* **96**, 56006 (2011).
- [34] S. Jungblut and C. Dellago, Heterogeneous crystallization on pairs of pre-structured seeds, *J. Phys. Chem. B* **120**, 9230 (2016).
- [35] S. van Teeffelen, C. N. Likos, and H. Löwen, Colloidal Crystal Growth at Externally Imposed Nucleation Clusters, *Phys. Rev. Lett.* **100**, 108302 (2008).
- [36] J. P. Hoogenboom, D. Derks, P. Vergeer, and A. van Blaaderen, Stacking faults in colloidal crystals grown by sedimentation, *J. Chem. Phys.* **117**, 11320 (2002).
- [37] A. van Blaaderen, R. Ruel, and P. Wiltzius, Template-directed colloidal crystallization, *Nature (London)* **385**, 321 (1997).
- [38] D. L. J. Vossen, A. van der Horst, M. Dogterom, and A. van Blaaderen, Optical tweezers and confocal microscopy for simultaneous three-dimensional manipulation and imaging in concentrated colloidal dispersions, *Rev. Sci. Instrum.* **75**, 2960 (2004).
- [39] F. Walton and K. Wynne, Using optical tweezing to control phase separation and nucleation near a liquid-liquid critical point, *Soft Matter* **15**, 8279 (2019).
- [40] M. Hermes, E. C. M. Vermolen, M. E. Leunissen, D. L. J. Vossen, P. D. J. van Oostrum, M. Dijkstra, and A. van Blaaderen, Nucleation of colloidal crystals on configurable seed structures, *Soft Matter* **7**, 4623 (2011).
- [41] C. Dellago, P. Bolhuis, and P. L. Geissler, Transition path sampling, *Adv. Chem. Phys.* **123**, 1 (2002).
- [42] T. S. van Erp and P. G. Bolhuis, Elaborating transition interface sampling methods, *J. Comput. Phys.* **205**, 157 (2005).
- [43] T. S. van Erp, Reaction Rate Calculation by Parallel Path Swapping, *Phys. Rev. Lett.* **98**, 268301 (2007).
- [44] J. Rogal, W. Lechner, J. Juraszek, B. Ensing, and P. G. Bolhuis, The reweighted path ensemble, *J. Chem. Phys.* **133**, 174109 (2010).
- [45] S. M. Foiles, M. I. Baskes, and M. S. Daw, Embedded-atom-method functions for the fcc metals Cu, Ag, Au, Ni, Pd, Pt, and their alloys, *Phys. Rev. B* **33**, 7983 (1986).
- [46] S. Plimpton, Fast parallel algorithms for short-range molecular dynamics, *J. Comput. Phys.* **117**, 1 (1995).
- [47] See Supplemental Material at <http://link.aps.org/supplemental/10.1103/PhysRevLett.128.166001> for a detailed description of computational details for MD and TIS simulations and additional distributions obtained from the RPE, which includes Refs. [48–51].
- [48] J. J. Hoyt, D. Olmsted, S. Jindal, M. Asta, and A. Karma, Method for computing short-range forces between solid-liquid interfaces driving grain boundary premelting, *Phys. Rev. E* **79**, 020601(R) (2009).
- [49] C. Dellago, P. G. Bolhuis, F. S. Csajka, and D. Chandler, Transition path sampling and the calculation of rate constants, *J. Chem. Phys.* **108**, 1964 (1998).
- [50] J. Bokeloh, R. E. Rozas, J. Horbach, and G. Wilde, Nucleation Barriers for the Liquid-To-Crystal Transition in Ni: Experiment and Simulation, *Phys. Rev. Lett.* **107**, 145701 (2011).
- [51] P. G. Bolhuis, Rare events via multiple reaction channels sampled by path replica exchange, *J. Chem. Phys.* **129**, 114108 (2008).
- [52] P. J. Steinhardt, D. R. Nelson, and M. Ronchetti, Bond-orientational order in liquids and glasses, *Phys. Rev. B* **28**, 784 (1983).
- [53] S. Auer and D. Frenkel, Numerical simulation of crystal nucleation in colloids, *Adv. Polym. Sci.* **173**, 149 (2005).
- [54] W. Lechner and C. Dellago, Accurate determination of crystal structures based on averaged local bond order parameters, *J. Chem. Phys.* **129**, 114707 (2008).